The Journal of Supercritical Fluids 172 (2021) 105194

Contents lists available at ScienceDirect

The Journal of Supercritical Fluids

journal homepage: www.elsevier.com/locate/supflu

Fast decellularization process using supercritical carbon dioxide for trabecular bone

Marta M. Duarte[a], Nilza Ribeiro[a,b], Inês V. Silva[a], Juliana R. Dias[c], Nuno M. Alves[c], Ana L. Oliveira[a,*]

[a] CBQF – Centro de Biotecnologia e Química Fina, Laboratório Associado, Escola Superior de Biotecnologia, Universidade Católica Portuguesa, 4200–375 Porto, Portugal
[b] DEMC – Departamento de Engenharia de Materiais e Cerâmica, Universidade de Aveiro, 3810–193 Aveiro, Portugal
[c] CDRSP – Centre for Rapid and Sustainable Product Development, Polytechnic Institute of Leiria, 2430–028 Marinha Grande, Portugal

HIGHLIGHTS

- Tri(n-butyl)phosphate and supercritical CO_2 are combined to decellularize bone.
- Treatments using Tri(n-butyl) phosphate led to a higher extraction of DNA content.
- The combined protocol led to a decrease in DNA content by at least 90%.
- Bone samples maintained mechanical integrity through all tested treatments.

GRAPHICAL ABSTRACT

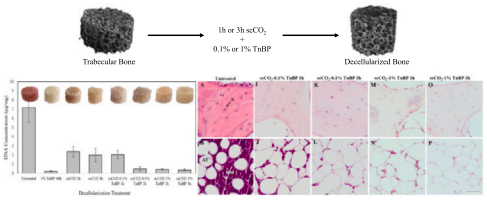

ARTICLE INFO

Keywords:
Decellularization
Supercritical carbon dioxide
TnBP
Trabecular bone

ABSTRACT

Decellularization is a process that consists on the removal of immunogenic cellular material from a tissue, so that it can be safely implanted as a functional and bioactive scaffold. Most decellularization protocols rely on the use of harsh chemicals and very long washing processes, leading to severe changes in the ultrastructure and loss of mechanical integrity. To tackle these challenges, supercritical carbon dioxide ($scCO_2$) is herein proposed as an alternative methodology for assisting decellularization of porcine trabecular bone tissue and is combined, for the first time, with Tri(n-butyl) phosphate (TnBP). Histological and DNA analysis revealed that both TnBP and $scCO_2$ were able to extract the DNA content from the scaffolds, being this effect more pronounced in treatments that used TnBP as a co-solvent. The combined protocol led to a decrease in DNA content by at least 90%, demonstrating the potential of this methodology and opening new possibilities for future optimizations.

1. Introduction

The rise of chronic disease worldwide has led to an increased interest in the development of new therapies that focus on restoring normal tissue function through transplantation of injured tissue with biomedically engineered smart matrices [1]. As such, decellularization, a process that consists in the removal of immunogenic cellular material from a tissue or organ, leaving behind the extracellular matrix (ECM), has become an appealing methodology. By using this method, it is possible to create functional and bioactive scaffolds, with the complexity and advantages provided by the native ECM, without the immunogenic drawbacks of transplantation of unprocessed tissue or organs.

There are multiple challenges inherent to the process of decellularization. First, there is an over-reliance on the use of harsh chemicals to achieve acceptable standards of cell removal, which have a very detrimental effect on the ECM and can lead to the disruption of its

Abbreviations: $scCO_2$, supercritical carbon dioxide; TnBP, tri(n-butyl) phosphate; ECM, extracellular matrix; GAGs, glycosaminoglycans

* Corresponding author.
E-mail address: aloliveira@porto.ucp.pt (A.L. Oliveira).

https://doi.org/10.1016/j.supflu.2021.105194
Received 3 December 2020; Received in revised form 26 January 2021; Accepted 7 February 2021
Available online 16 February 2021

ultrastructure and mechanical properties. The use of detergents has also been linked to losses of collagen, elastin, and glycosaminoglycans (GAGs), leading to an altered ultrastructure and a loss of mechanical integrity [2,3]. Furthermore, most protocols rely on immersion and agitation, and/or require long washes to remove any potentially toxic agent used during the decellularization process. This can lead to protocols that can take up to several days to be completed [4].

To tackle these challenges, supercritical carbon dioxide ($scCO_2$) has been proposed as a new alternative methodology for assisting decellularization [5]. CO_2 can achieve its critical point at relatively low temperature and pressure (31.1 °C and 7.39 MPa), which allows for its use with biological tissues, and it has a high transfer rate and permeability, resulting in a faster decellularization process [5]. $scCO_2$-assisted decellularization can be used to replace or diminish the exposure of harsh chemicals such as detergents, which in turn could lead to better preservation of the ECM's biochemical and mechanical properties. In specific, the possibility of using $scCO_2$ to induce cellular death and removal without the use of aggressive surfactant solutions, or to help specific decellularization agents to achieve greater penetration of tissues, has been explored [5–7]. Additionally, $scCO_2$ treatment can be used to simultaneously remove both cellular content and any potentially toxic co-solvent utilized during decellurization [6–8]. To this date, $scCO_2$ has already been used to aid decellularization of several tissue grafts (Table 1), such as aorta [5,6,9], pericardium [10], myocardium [11], pulmonary arteries [12], cornea [9,11,13], tendons [7,14], adipose tissue [15], optic nerve [11], skin [7,16], cartilage [7], and bone [8,17].

Furthermore, $scCO_2$ has already been used for bone delipidation [18,19], and sterilization [20,21], with minimal alterations to both cancellous and trabecular bone biomechanical properties. These studies show the potential of $scCO_2$ processing to create decellularized bone scaffolds.

The main objective of this work is to investigate innovative strategies to obtain faster and more effective decellularization protocols while avoiding the use of harsh agents such as detergents. The present work proposes a new methodology for the decellularization of trabecular bone using $scCO_2$ technology combined with Tri(n-butyl) phosphate (TnBP). $ScCO_2$-assisted decellularization is expected to lead to a faster decellularization process, therefore reducing the period in which the tissue is exposed to TnBP. To our knowledge, TnBP is herein proposed for the first time as an alternative to harsh chemicals such as detergents. TnBP is an organophosphorus compound currently used as an extractant and plasticizer. It forms stable hydrophobic complexes with some metals, disrupting protein-protein interactions, thus facilitating the removal of cells. For decellularization of denser tissues, such as tendon, TnBP was demonstrated to be more effective than Triton X-100 detergent, at removing cell nuclei [3]. Furthermore, the use of TnBP did not significantly impacted the tissue's structure and composition [23], while the use of detergents compromised its integrity [3,24].

These properties make TnBP an appealing alternative to the use of detergent or alcohol. To conjugate it with $scCO_2$ constitutes a breakthrough strategy to promote decellularization for the creation of a functional biological scaffold from trabecular bone tissue. For this purpose, trabecular bone was here used as one of the most challenging models for testing for the first time our proposed decellularization routes. Three different protocols were implemented: the use of TnBP aqueous solution; simple $scCO_2$ treatment, and $scCO_2$ treatment using TnBP as co-solvent. Due to the innovative nature of this study, several concentrations of co-solvent and time variants to protocols were implemented to investigate any possible harmful effects caused by prolonged exposure to $scCO_2$ treatment.

To the authors' knowledge, there have been no other studies reporting on the effects of TnBP on bone tissue. On the other hand, the combination of this compound with $scCO_2$ has also not been reported in the literature for bone tissue or otherwise.

2. Materials and methods

2.1. Animal tissue processing

Femurs from freshly slaughtered (< 24 h) female pigs were obtained from a local slaughterhouse. The distal ends of the femurs were cut into slices approximately 3–4 millimeters tall using a band saw machine. The bones were transported to the laboratory properly conditioned and refrigerated to prevent tissue degradation. Afterward, the slices were cut into small cylindrical pieces (Ø 6 mm) using a biopsy punch (Kai Medical, Japan). Any piece containing articular or subchondral elements were immediately discarded. Samples were then rinsed 3 times with deionized water before being frozen at −20 °C until further use.

2.2. Cell lysis treatment

A freeze-thaw step was done to induce cell lysis in bone samples before the decellularization treatment. Initially, samples were thawed at room temperature (RT) for 30 min and rinsed 3 times with deionized water. Afterward, the bone pieces underwent six cycles of rapid freeze-thaw, each comprising of a freezing step in liquid nitrogen (–196 °C) for 2 min and a rapid melting step in a water bath at room temperature for 5 min. Lastly, samples were rinsed 3 times in deionized water.

To study the effects of the freeze-thaw treatment, 2 samples were immediately put in a formaldehyde solution for further histological analysis via hematoxylin and eosin (H&E) staining, and another 2 samples were immersed in a fixing solution (4% glutaraldehyde and 6% formaldehyde) for later examination via transmission electron microscopy (TEM). The remaining samples were frozen at –20 °C until further use.

2.3. Decellularization

Three different approaches to decellularize trabecular bone tissue were analyzed in this work: i) immersion in tri-n-butyl phosphate (TnBP); ii) supercritical CO_2 treatment; and iii) a combined $scCO_2$-TnBP treatment. In total, seven different protocols (Fig. 1) were implemented and examined: 1% (v/v) TnBP solution treatment for 48 h (this concentration was described to be effective in decellularize tendon tissue in Cartmell and Dunn's work [3]), $scCO_2$ treatment for 1 and 3 h, $scCO_2$ treatment with 0.1% (w/v) TnBP for 1 and 3 h, and $scCO_2$ treatment with 1% (w/v) TnBP for 1 and 3 h.

2.3.1. TnBP treatment

The TnBP treatment was adapted from a protocol by Cartmell et al. [3]. Bone samples were incubated with 1% (v/v) TnBP for 48 h under continuous agitation (230 rpm). The solution was changed after 24 h.

Afterward, the samples were rinsed in deionized water 3 times and washed for 30 min in deionized water under continuous agitation. Representative samples (n = 2) were set immediately aside and immersed in a formaldehyde solution for H&E staining. The remaining samples were frozen at –20 °C until further use.

2.3.2. $scCO_2$ treatment

Samples were sealed in sterilization pouches (Tyvek, USA) and placed inside the pressure vessel of a Parr Instruments series 4540 high-pressure reactor (Parr Instrument Company, Illinois, USA). Premium CO_2 Liquid Premier with 99.995% of purity (Gasin Air Products, Portugal) was introduced into the pressure vessel via a high-pressure pump at 50 g/min and the pressure was set to 24 MPa. The temperature was adjusted to 40 °C and the rotation motor speed was set at 600 rpm. Pressurization took approximately 30 min to complete. After 1 or 3 h, the vessel was slowly depressurized using a manually operated valve. Depressurization took approximately 25 min to complete.

After treatment, the samples were subjected to the same washing and storage procedures as described in Section 2.3.1.

Table 1
Compilation of the most relevant works regarding $scCO_2$-assisted decellularization of several biological tissues.

Tissue	References	$scCO_2$ conditions	Pretreatment	Comments
Aorta	[5]	15 MPa, 37 °C, 1 h + ethanol	No pretreatment	- Cell nucleus were removed from the aorta within 20 min; - No decrease in mechanical strength was observed;
	[6]	10.3 or 27.6 MPa, 37°C, 1 h + water/ethanol	0.1% SDS, 48 h	- Hybrid SDS-$scCO_2$ treatment reduced DNA content by ~98%; - $scCO_2$-ethanol without SDS pretreatment resulted in an DNA reduction of ~81%; - Adding water to the pressure vessel reduced water extraction during $scCO_2$ processing, reducing tissue stiffness compared to $scCO_2$-ethanol samples;
	[9]	17.2 MPa, 37°C, 1 h + ethanol	No pretreatment	- $scCO_2$-ethanol treatment reduced DNA content by ~84%; - $scCO_2$ treatment at 17.2 MPa preserved the ECM's architecture;
Pericardium	[10]	10 MPa, 35°C, 1 h	25 wt% H_2O_2 + 1.25 M NaOH + 0.1 M H_3PO_4	- $scCO_2$ treatment preserved the tissue's ultimate tensile strength; - $scCO_2$-treated samples met the mechanical requirements for use in cardio-thoracic surgery;
Myocardium	[11]	3. 17.2 MPa, 37°C, 1 h + ethanol	5 freeze-thaw cycles 1.5 M NaCl, 12 h	- $scCO_2$-ethanol treatment reduced DNA content by ~60%; - $scCO_2$-ethanol treatment preserved ~64% of GAG content; - ECM structure was preserved;
Heart	[22]	35 MPa, 37°C, 6 h + ethanol	No pretreatment	- $scCO_2$-ethanol treatment reduced DNA content by ~96%; - $scCO_2$-treated samples contained more ECM components (collagen, GAGs, laminin, angiogenic factors, etc) than detergent-treated samples;
Pulmonary artery	[12]	15–30 MPa, 37–40 °C, 90–120 min + limonene	1 freeze-thaw cycle	- Pressurized CO_2-limonene with additional enzyme treatment reduced DNA content by ~93%; - Pulmonary ECM was preserved after decellularization;
Cornea	[13]	35 MPa, 45 °C, 80 min + ethanol	2 M NaCl, 30 min Ultrapure water for 30 min	- $scCO_2$-ethanol treatment reduced DNA content by ~75%; - $scCO_2$-treated corneas showed good transparency and biocompatibility;
	[11]	17.2 MPa, 37 °C, 1 h + ethanol	No pretreatment	- $scCO_2$-ethanol treatment reduced DNA content by ~82%;
	[9]	13.8–9.7 MPa, 37 °C, 20 min + ethanol	No pretreatment	- Histological analysis showed significant cell removal after $scCO_2$-ethanol treatment; - $scCO_2$-ethanol processing at 13.8 MPa was effective in preserving the ECM;
Optic nerve	[11]	17.2 MPa, 37 °C, 4 h + ethanol	1 freeze-thaw cycle 0.5% EDTA, 24 h	- $scCO_2$-ethanol treatment reduced DNA content by ~54%; - The integrity of the ECM was well preserved;
Tendon	[7]	25 MPa, 37 °C, 1 h + LS-54	No pretreatment	- $scCO_2$-detergent treatment reduced DNA content by ~67%; - GAG content was significantly reduced; - No significant difference found in the tendon's stiffness;
	[14]	10.2 MPa, 39 °C, 2 h + SDS	0.1% EDTA, 4 h	- $scCO_2$-SDS treatment was not able to thoroughly decellularize tendons; - The $scCO_2$-SDS protocol preserved the mechanical integrity of the tendons;
Skin	[7]	25 MPa, 37 °C, 1 h + Ls-54	1 M NaCl, 24 hEpidermis removal	- $scCO_2$-detergent treatment reduced DNA content by ~95%; - GAG content was significantly reduced; - Cell adhesion molecules were preserved in the ECM;
	[16]	20–35 MPa, 30–50 °C, 40 min + ethanol	Epidermis removal	- $scCO_2$-decellularized ADM scaffolds showed no obvious nucleus and DNA - scaffolds enhanced cell proliferation and regeneration in diabetic wounds;
Cartilage	[7]	25 MPa, 37 °C, 1 h + Ls-54	6 freeze-thaw cycles	- $scCO_2$-detergent treatment reduced DNA content by ~82%; - GAG content was significantly reduced; - Elastic modulus was significantly lower than control;
Bone	[8]	10–30 MPa, 50 °C, 30 min	0.1% Triton X-100, 2 h	- - Bone scaffold was not rejected after implantation;
Bone	[17]	30 MPa, 50 °C, 30 min	0.1% EDTA, 1 h 0.1% SDS, 6 h	- - Scaffold retained ECM microstructures and components; - - Scaffold supported the proliferation of MSCs;

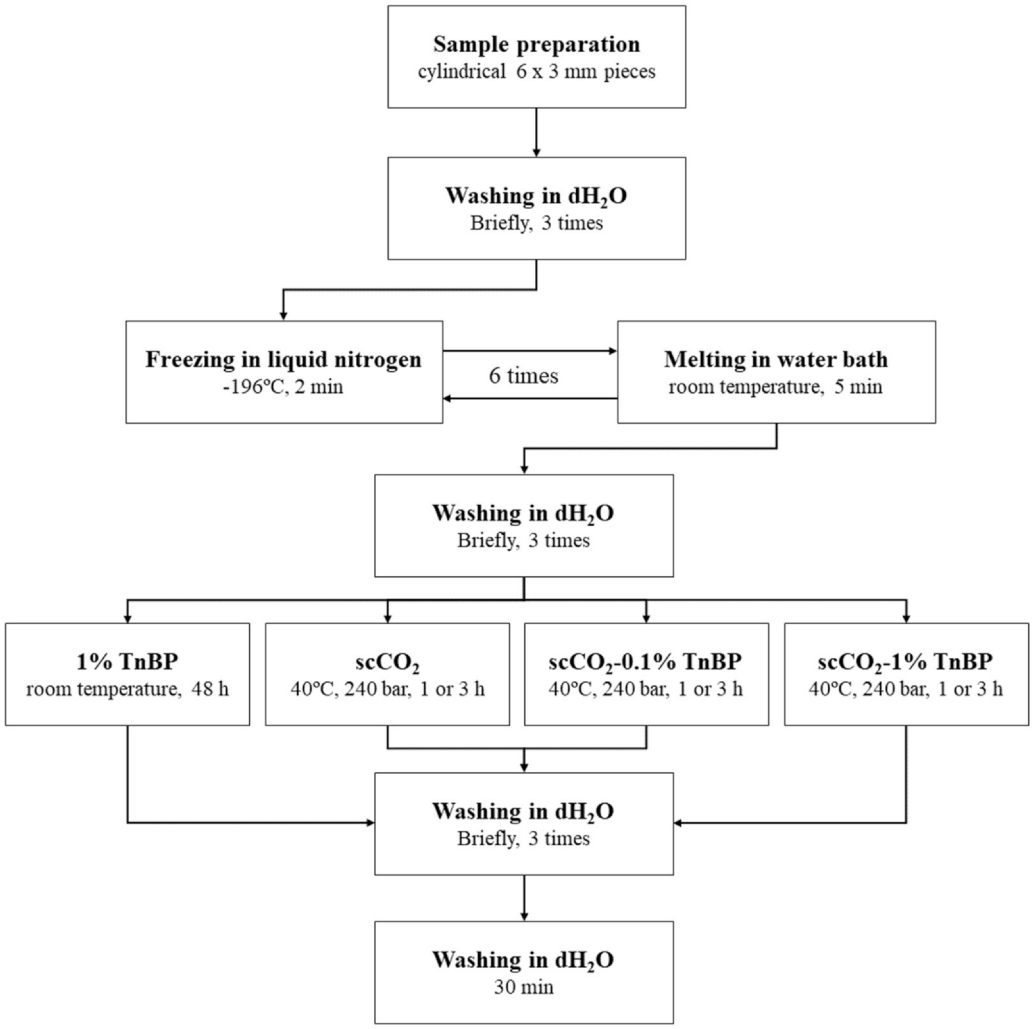

Fig. 1. Decellularization Methodology: Flow-chart detailing the decellularization process and protocol variants. Samples were subjected to one of three different treatment types: TnBP for 48 h, $scCO_2$ for 1 h or 3 h, $scCO_2$-0.1% TnBP for 1 h or 3 h, and $scCO_2$-1% TnBP for 1 h or 3 h. In total, seven different protocols were examined.

2.3.3. $scCO_2$-TnBP treatment

The $scCO_2$-TnBP treatment followed the conditions described in Section 2.3.2. with the addition of 0.1% or 1% (w/v) TnBP (Merck Millipore) into the pressure vessel before $scCO_2$ treatment.

2.4. Transmission electron microscopy

Transmission Electron Microscopy (TEM) was used to confirm if cell lysis had been successfully induced after freeze-thaw treatment. Samples were fixed via immersion in 2.5% (v/v) glutaraldehyde and 2% (v/v) paraformaldehyde in 0.1 M sodium cacodylate buffer (pH 7.4) solution for 5 days. Afterward, samples were washed and decalcified in MoL-DECALCIFIER (EDTA-based decalcifying solution) for 48 h and post-fixated in 2% (v/v) osmium tetroxide in 0.1 M sodium cacodylate buffer (pH 7.4) solution for 2 h. Samples were then incubated with 1% (v/v) uranyl acetate O/N, washed in buffer and dehydrated through a graded series of ethanol, and finally embedded in Epon (EMS). Ultrathin sections were cut at 50 nm and prepared on an RMC Ultramicrotome (PowerTome, USA) using a diamond knife and recovered to 200 mesh Formvar Ni-grids, followed by 2% (w/v) uranyl acetate and saturated lead citrate solution. Visualization was performed at 80 kV in a JEM-1400 microscope (JEOL, Japan) and digital images were acquired using a CCD digital camera Orious 1100 W (Japan) using 8000x and 12,000x magnifications.

2.5. Micro-computed tomography

Control and treated samples were scanned in a Skyscan 1174 (Brucker, USA) with an image pixel size of 9.55 μm, exposure time of 8500 ms, and a rotation step of 0.9°. The three-dimensional reconstructions were made using CTan and CTvox, while the transversal plane views were made using Dataviewer. Porosity measurements (n = 5) were derived from Micro Computed Tomography (μ-CT) reconstructions.

2.6. Scanning electron microscopy

Samples were coated with Au/Pd with a sputter coater (Quorum Technologies, UK) for 45 s prior examination on a Vega3-LM scanning electron microscope (SEM) (TESCAN, Czech Republic). Visualization was performed at 15 kV and digital images (cross-sections) were acquired at 50x magnification.

2.7. Mechanical compression testing

Mechanical properties of treated and control samples (n = 6) were assessed via uniaxial compression testing using a texturometer equipment (TA.XT PLUS, Texture Analyzer, UK). Initially, the height of samples was measured using a 200 mm digital caliper (Mitutoyo, Japan) to allow for correction for the sample's geometry. Compression

was done using a 5 mm cylinder stainless probe (Stable Micro Systems Ltd, UK) and a 30 kg compression load cell. Testing was done using a crosshead speed of 1 mm/s until fracture or 90% elongation was reached. Results were obtained as a stress versus strain rate curve and subsequently analyzed in Microsoft Excel (Microsoft, USA). Young's modulus was derived from the slope of the stress-strain curve's linear portion, while the yield point was obtained from the first of the stress-strain curve's non-linear portion.

2.8. Histology

For tissue fixation, bone samples were previously fixed in 10% (v/v) buffered formalin for a minimum of 24 h and decalcified in EDTA for 48 h. Samples were then routinely processed in an automated system and embedded in paraffin using a Microm STP-120 spin tissue processor (Thermo Scientific, USA). Sequential sections for hematoxylin and eosin staining were made at 4 μm in adhesive slides using a Shandon Finesse 325 (Thermo Scientific, USA).

2.9. DNA quantification

DNA content was analyzed from control and treated bone samples (n = 5) to access decellularization efficiency. Samples were frozen in liquid nitrogen (−196 °C) and ground into small particles using a mortar and pestle. PureLink™ Genomic DNA Mini Kit (Thermo Fisher Scientific, USA) was used to extract genomic DNA from known masses of bone samples following the manufacturer's protocol. DNA yield was then measured using a microplate spectrophotometer (BioTek, USA) by UV absorbance at 260 nm using the following equations:

$$\text{Concentration}(\mu g/ml) = A_{260} \times \textit{Dilution Factor} \times 50\ \mu g/ml \quad (2.9.1)$$

$$\text{DNA yield}(\mu g) = \textit{Concentration}(\mu g/ml) \times \textit{Total Sample Volume}\ (ml) \quad (2.9.2)$$

2.10. Statistical analysis

Statistical analysis was conducted using IBM® SPSS® Statistics (International Business Machines Corporation, USA). Significant differences were identified at $p \leq 0.05$ using independent samples *t*-tests.

3. Results

3.1. Assessment of cell lysis

In Fig. 2 are presented the macroscopic field pictures and TEM micrographs close-ups of untreated samples (Fig. 2a,c) and samples subjected to the cell lysis treatment (Fig. 2b,d). Macroscopic analysis of the samples' morphology revealed no significant differences in color, shape, or texture between untreated samples (Fig. 2a) and samples that had been subjected to the cell lysis treatment (Fig. 2b).

Transmission electron micrographs showed significant differences between cells within untreated samples (Fig. 2c), and those present in samples subjected to the rapid freeze-thaw treatment (Fig. 2d). The cells observed in untreated samples exhibited a normal morphology with outlined cell components, while no such distinctions were found in the cells from treated samples. In the latter, most of the cytoplasm was eliminated from these cells and cells were shrunken and smaller than cells found in untreated samples. This morphology has been associated with non-viable bone cells after freeze-thaw treatment [25]. These results demonstrate that the treatment proposed was successful in inducing cell lysis.

3.2. Integrity and structure of decellularized bone

Fig. 3 presents the macroscopic images of untreated trabecular bone samples and samples subjected to one of the following decellularization protocols: 1% TnBP for 48 h, $scCO_2$ for 1 h and 3 h, $scCO_2$-0.1% TnBP treatment for 1 h and 3 h, and $scCO_2$-1% TnBP treatment for 1 h and 3 h. The untreated bone samples had an intense red color and a uniform texture (Fig. 3a). All samples exhibited some degree of discoloration after being subjected to their respective treatments. However, this loss of color was less pronounced for the sample subjected to $scCO_2$ for 1 h (Fig. 3c). As for the samples subjected to the hybrid $scCO_2$-TnBP treatment (Fig. 3e, f, g, h), the extent of discoloration was higher than $scCO_2$ treatment but lesser than the samples treated with 1% TnBP for 48 h, which exhibited a pure white color. Texture appeared to be similar between all samples.

Micro-CT revealed similar microarchitecture between untreated and treated samples (Fig. 4 and 5). Changes to the microstructure were observed in the samples subjected to $scCO_2$ treatment for 3 h and $scCO_2$-0.1% TnBP for 3 h, as the trabeculae appeared to be more open (Fig. 5d,f), as compared to their 1-hour counterparts (Fig. 5c,e). Porosity measurements derived from Micro-CT imaging are presented in Table 2. Porosity measured in treated bone samples was higher than in untreated samples.

SEM micrographs clearly show the porous complex network of the bone extracellular matrix for untreated and treated samples (Fig. 6). The micrographs of untreated samples showed that the marrow spaces appear to be filled with marrow content, partially obscuring the pores from view (Fig. 6a), unlike the treated samples where these pores are more easily observable (Fig. 6b-h).

Table 3 shows the data obtained from mechanical compression testing for Young's modulus, strength, elongation at yield, and elongation at break. A significant increase in Young's modulus was observed in samples subjected to all treatments, except for those subjected to $scCO_2$-1% TnBP for 3 h. Ultimate strength was significantly superior in all treated samples compared to untreated. The ductility of the samples suffered significant alterations for samples subjected to 1% TnBP for 48 h, $scCO_2$ for 3 h, $scCO_2$-0.1% TnBP for 3 h, and both $scCO_2$-1% TnBP treatments.

3.3. Extent of cell removal

Hematoxylin and eosin (H&E) staining of representative sections of untreated and treated samples are presented in Fig. 7. Two sections are shown for each treatment type: a section focusing on the trabeculae (Fig. 7a, c, e ,g, i, k, m, o) and another focusing on the marrow spaces (Fig. 7b, d, f, h, j, l, n, p). As shown in Fig. 7, the extracellular matrix of the untreated tissue stained pink, and cell nuclei stained a dark purple. For all treatments, some degree of cell removal was observed (Fig. 7c–p). Cell removal was more extensive in treatments that used TnBP (Fig. 7g–p) as compared to treatments that only used $scCO_2$ (Fig. 7c–f). No treatment was able to remove completely cellular material that was embedded within the trabeculae.

DNA concentration values for untreated and treated samples are presented in Fig. 8 and Table 4. The results revealed that there was a general decrease of DNA content for all treated samples, which was more pronounced for samples subjected to 1% TnBP for 48 h, $scCO_2$-0.1% TnBP 3 h, and both $scCO_2$-1% TnBP treatments.

4. Discussion

The main objective of this work was to investigate and compare the potential of three innovative protocols to decellularize trabecular bone tissue without the use of harsh agents such as detergents. For this purpose, an adaptation of Cartmell and Dunn's protocol [3] was used for the first time on a bone tissue type. This protocol has been previously used to successfully decellularize tendons from rat tails, using a 48 h immersion period in 1% (v/v) TnBP solution. Additionally, the effects of the use of supercritical carbon dioxide as a decellularization agent were also investigated, without the addition of any *entrainer* or secondary agent. Finally, a combined decellularization strategy using supercritical carbon dioxide and TnBP was herein proposed and

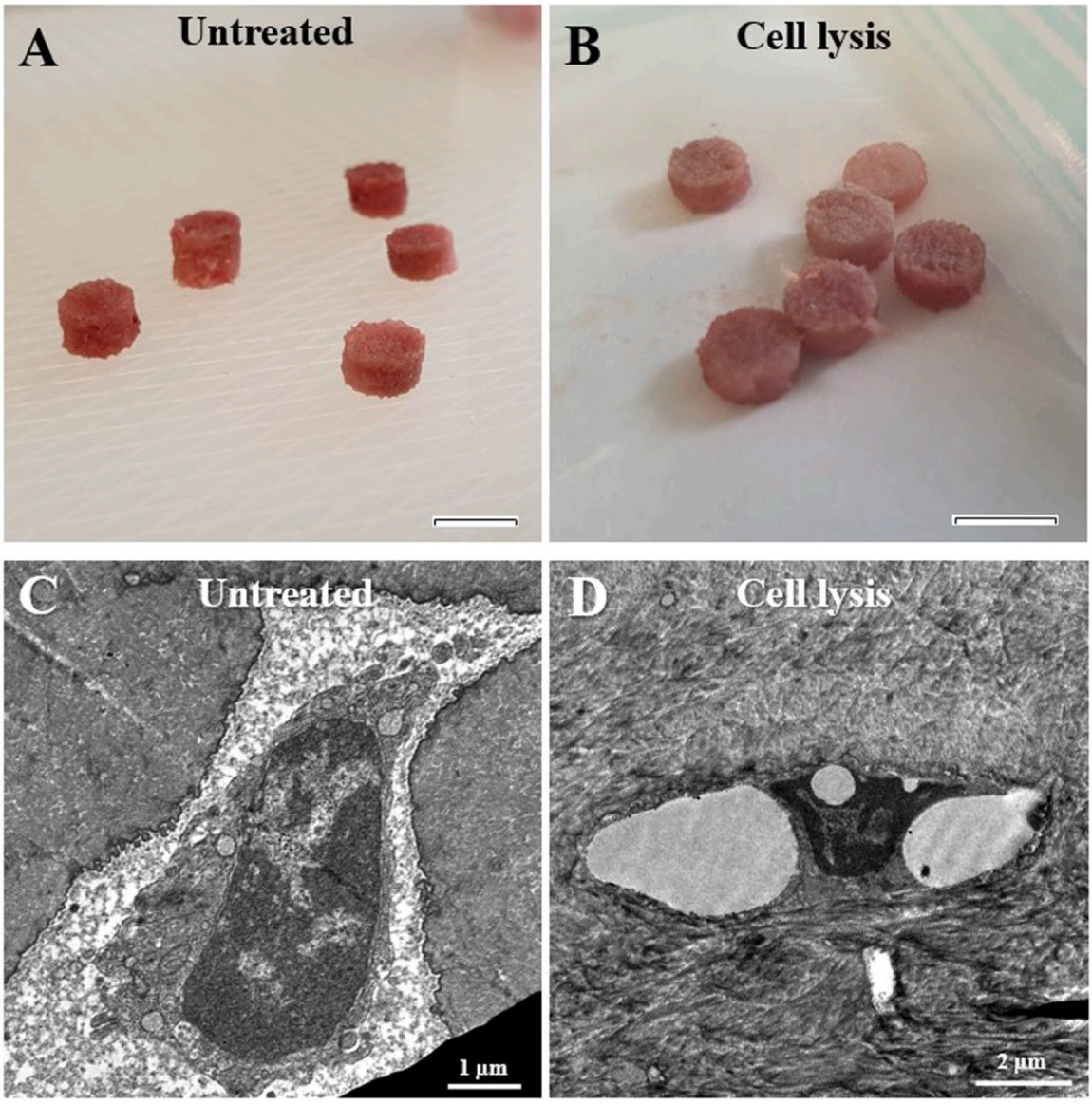

Fig. 2. Cell Lysis Treatment: Up: Macroscopic field photographs of (A) untreated samples and (B) samples subjected to cell lysis treatment. Scale bar indicates 6 mm. Bottom: TEM micrographs of osteocytes of (C) untreated sample (12,000x) and (D) sample subjected to cell lysis treatment (8,000x). Scale bars indicate 1 µm in (C) and 2 µm in (D).

studied. While $scCO_2$ has been previously used to aid in the decellularization of bovine bone, this protocol also involved the use of Triton X-100, a non-ionic detergent that is known to disrupt the ultrastructure of ECMs [8,26]. Additionally, different testing periods of both the $scCO_2$-TnBP and $scCO_2$ methods were assessed to investigate any possible degradation effects on the extracellular matrix caused by prolonged exposure to $scCO_2$ treatment.

4.1. The importance of cell lysis

The induction of cell lysis is usually the first step in a decellularization protocol [27]. Freeze-thawing processing was chosen since it has been proven to lyse cells from several tissues without severely impacting ECM composition and ultrastructure [26]. The intracellular ice crystals that form during rapid freezing disrupt cell membranes, leading to their collapse. This method is also believed to cause minimal impact on mechanical properties for load-bearing tissues, an essential factor for creating a scaffold to serve as a bone graft substitute [26,28]. Specifically, for the decellularization of bone, freeze-thawing appears to be a well-accepted initial step [29–31]. In the case of $scCO_2$-assisted decellularization, some studies have reported successful decellularization using $scCO_2$ with an additional co-solvent (such as ethanol) [5,9], while others could not reproduce these results [6,7]. Casali et al. [6] suggested that $scCO_2$ may be unable to properly permeate the cell membrane, leading to incomplete cell removal. While the mechanism behind $scCO_2$ decellurization is still unexplored, studies examining the mechanism behind $scCO_2$ sterilization seem to suggest that $scCO_2$ can penetrate and cause damage to the cell membrane [32,33], however the extend of this damage appears to be insufficient to lead to a successful a decellurization. As such, in this work, a rapid freeze-thawing methodology adapted from Abedin et al.'s work was taken into account to induce cell lysis before decellularization [30]. In the present study, no significant changes in the color or structure of the samples were observed after they were subjected to the cell lysis treatment, suggesting some degree of tissue preservation.

4.2. Impact of decellularization on bone properties

The extracellular matrix of trabecular bone has a complex microarchitecture with a high surface area, which is important for efficient

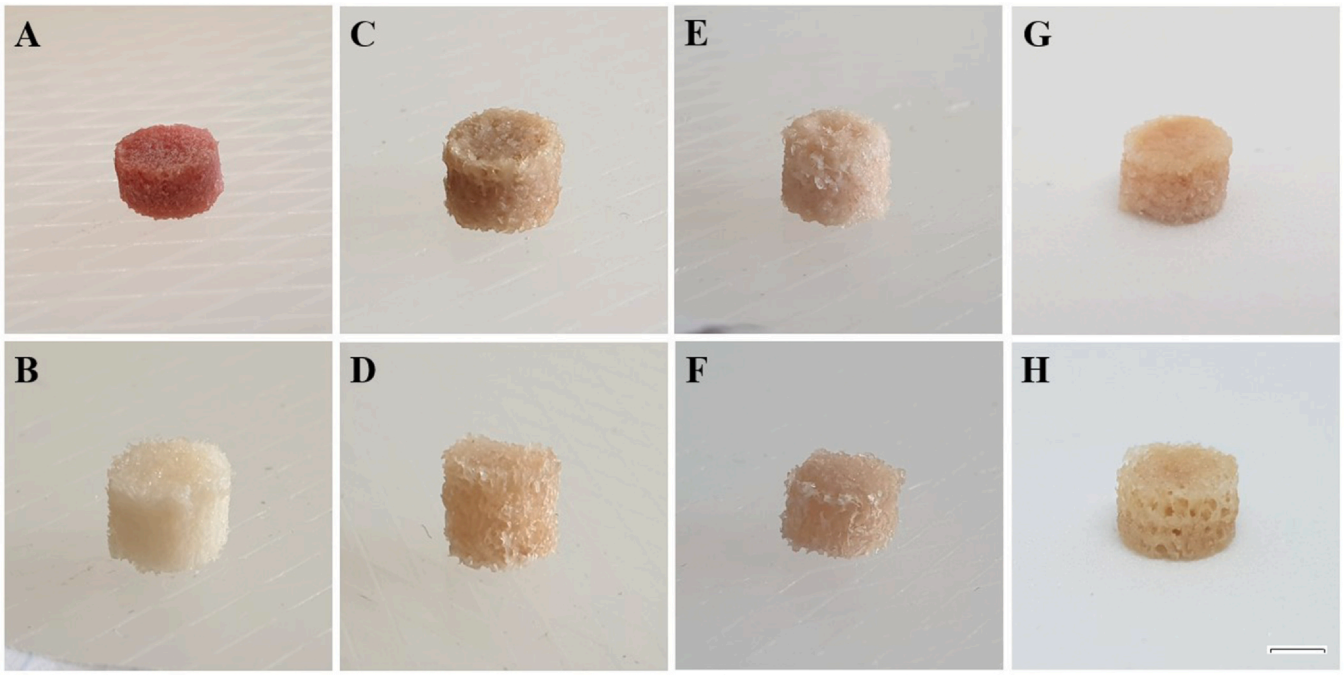

Fig. 3. Trabecular Bone Samples: Macroscopic Field Images of (A) Untreated sample; (B) 1% TnBP treatment for 48 h; $scCO_2$ treatment for 1 h (C) and (D) 3 h; $scCO_2$-0.1% TnBP treatment for 1 h **(E)** and **(F)** 3 h; $scCO_2$-1% TnBP treatment for 1 h (G) and (H) 3 h. Scale bar indicates 3 mm.

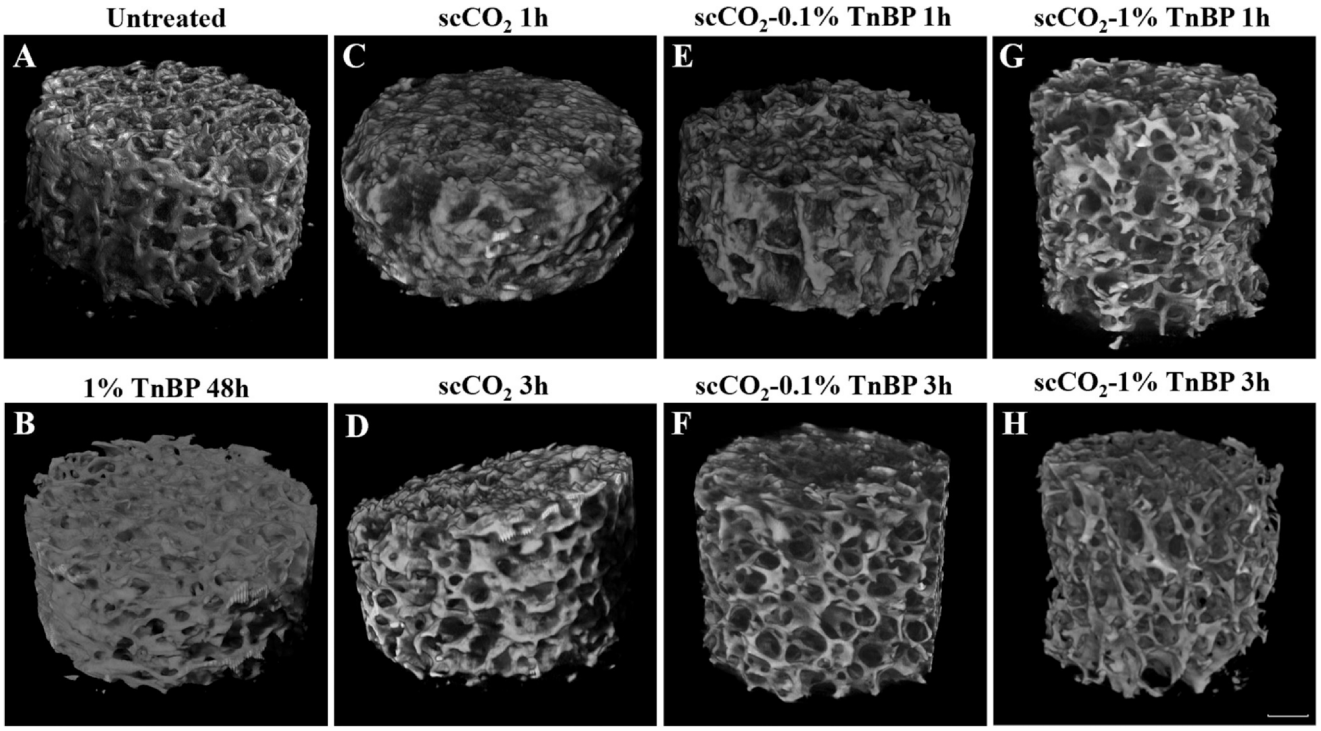

Fig. 4. 3-dimensional projections: Micro-CT generated 3-dimensional projections of (A) Untreated; (B) 1% TnBP for 48 h treatment; (C) $scCO_2$ treatment for 1 h and (D) 3 h; (E) $scCO_2$-0.1% TnBP treatment for 1 h and (F) 3 h, (G) $scCO_2$-1% TnBP treatment for 1 h and (H) 3 h. Scale bar indicates 1 mm.

nutrient and growth factor diffusion [34]. Not only does bone architecture plays a role in the osteogenic differentiation, but it also impacts the final mechanical properties of bone, which is why any scaffold used as a bone substitute should mimic these properties [34–36]. The pore size can have a significant effect on osteoblast survival and bone formation. Excessively small pore sizes can lead to decreased oxygen and nutrient diffusion, affecting osteoconductivity, therefore larger pore sizes (200–600 μm) are considered optimal for bone repair and regeneration [37]. Porosity in trabecular bone is also highly variable and can fluctuate between 50% and 90% depending on several factors, such as anatomic site, age, disease, or other interspecimen variations [38]. Otherwise, a porosity above 90% decreases the mechanical strength of the scaffold, so a careful balance between the need for adequate diffusion of nutrients and oxygen and the mechanical properties of the scaffold needs to be met for bone graft substitutes [34].

In this work, the complex architecture observed in untreated samples has been preserved for all treatments, although the surface topology of the samples subjected to 1% TnBP for 48 h appeared distinct

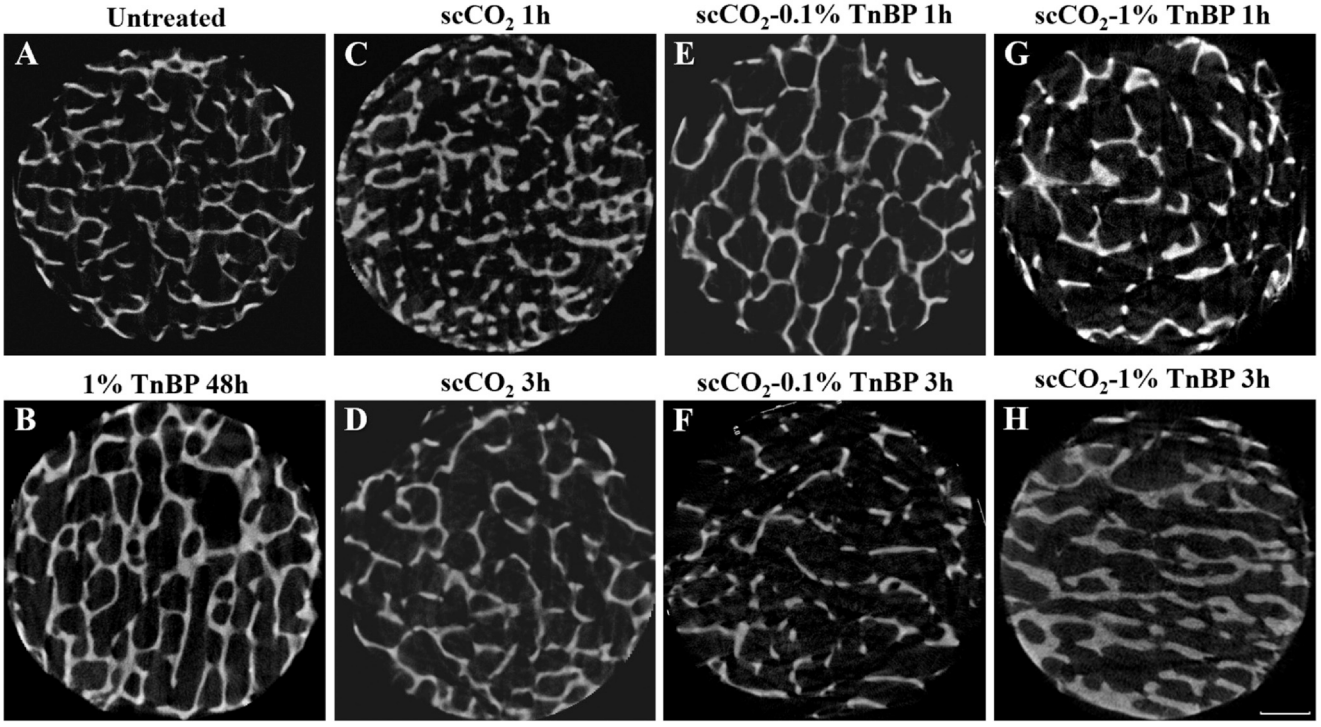

Fig. 5. Transversal Plane Views: Micro-CT generated transversal plane views of (A) Untreated; (B) 1% TnBP for 48 h treatment; (C) $scCO_2$ treatment for 1 h and (D) 3 h; (E) $scCO_2$-0.1% TnBP treatment for 1 h and (F) 3 h, (G) $scCO_2$-1% TnBP treatment for 1 h and (H) 3 h. Scale bar indicates 1 mm.

Table 2
Porosity values for untreated and treated samples. Porosity is presented as mean ± standard deviation.

Treatment	Porosity (%)
Untreated	42.2 ± 1.62
1% TnBP 48 h	59.2 ± 4.69
$scCO_2$ 1 h	54.0 ± 9.34
$scCO_2$ 3 h	54.8 ± 5.59
$scCO_2$-0.1% TnBP 1 h	52.2 ± 7.15
$scCO_2$-0.1% TnBP 3 h	56.0 ± 2.19
$scCO_2$-1% TnBP 1 h	56.4 ± 6.45
$scCO_2$-1% TnBP 3 h	59.2 ± 4.69

from samples subjected to other treatments. As expected, the porosity of the samples increased with the degree of decellularization, due to the removal of cellular content from the extracellular matrix. Even so, the levels of porosity obtained for all treatments were within the range of porosity reported for trabecular bone tissue [34]. For the treatments $scCO_2$-1% TnBP (3 h) and 1% TnBP (48 h), the degree of porosity observed was similar to that described for the demineralized bone matrix (~62.24%) [39]. As expected, the porosity of the samples increased after decellularization.

This increase is due to the removal of cellular content from the porosity, and does not necessarily reflect a change to the microstructure of the pores. Indeed, in the SEM images for untreated samples (Fig. 6a) we can observe that the surface of the ECM appears to be covered material, which is compromising the porous architecture of trabecular bone. This is also observable for the sample treated with $scCO_2$ for 1 h (Fig. 6c), although to a much lesser degree than in the untreated samples, as pores are already observable in the structure. The complex microstructure of pores is easily observable in all other treatment groups (Fig. 6b, d–h). These results are similar to those of Ling et al. [17], although in the present work we could still observe some degree of residual cell content, since some of micropores still have a more rugged surface, instead of being completely smooth.

As discussed above, trabecular bone is one of the most heterogeneous biological tissues. Its biomechanical properties, like ultimate strength or elasticity modulus, can differ widely even within the same species, such as both within and across anatomical sites, after the advent of disease, or with age [40]. Even intra-specimen variations in tissue properties can have biomechanical consequences: variations in trabecular thickness, for example, can significantly alter the apparent modulus of bone [40]. For this reason, it can be difficult to establish a standard value of comparison when it comes to mechanical parameters such as Young's Modulus or Yield Stress. Studies have pointed out to values of around 50–389 MPa for Young's Modulus of human trabecular bone [41,42]. Porcine bone also appears to have modulus values similar to human bones, which is why it is a common alternative for bone grafting [42]. Yield stress and strength values in trabecular bone are also heterogeneous (varying with anatomic location, age, disease, among others), anisotropic (depend on loading direction), and asymmetric (compression versus shear) [40]. The values for Young's modulus found in this work were lower than those presented in the literature [41,42], which could be related to the non-standard sample geometry (cylindrical 6 × 3 mm pieces) used for mechanical compression testing. The geometry of trabecular bone specimens has been previously found to significantly impact their mechanical behavior [43,44]. However, since the same methodology was used to test untreated and treated samples, this study focused on the comparison between the values obtained through this work. The samples treated with 1% TnBP for 48 h had superior ultimate strength, Young's modulus, and elongation at yield as compared to untreated samples. TnBP has been known to damage collagen content according to some studies [26,45], yet the stiffness and ductility of the samples analyzed in this work were not negatively impacted. A significant difference in the elongation at yield was observed, marking an increase in the extensibility for these samples. In line with the works of Deeken et al. [24] and Xing et al. [46] developed on TnBP decellularized tendons. Deeken et al. [24] suggested that a possible reason for this increase was that the removal of cellular content from tissues allowed some degree of collagen crosslinking might have occurred during treatment. While the

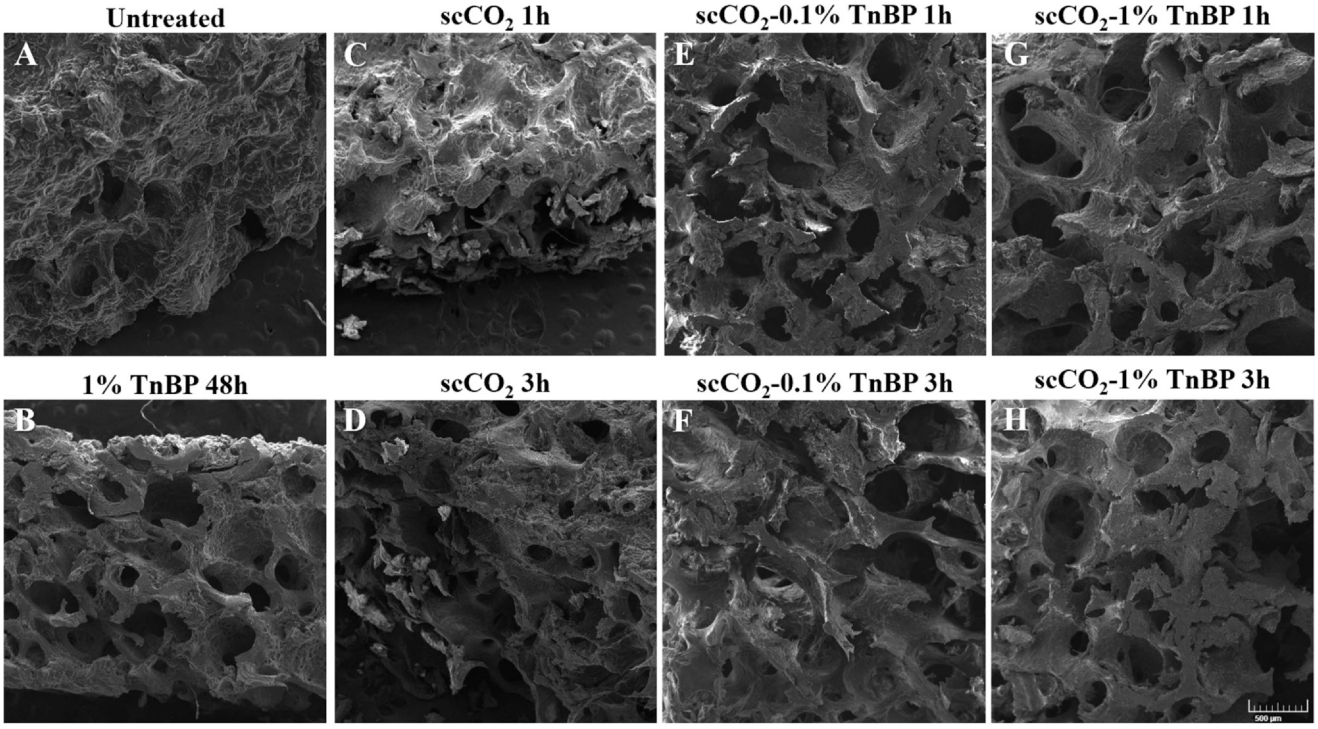

Fig. 6. SEM Micrographs of Bone Samples: Cross-sections of samples for each treatment type (50x) of (A) Untreated; (B) 1% TnBP treatment; (C) $scCO_2$ treatment for 1 h and (D) 3 h; (E) $scCO_2$-0.1% TnBP treatment for 1 h and (F) 3 h; (G) $scCO_2$-1% TnBP treatment for 1 h and (H) 3 h. The scale bar indicates 500 µm.

strength of bone depends mostly on its mineral phase, collagen crosslinking can affect the post-yield mechanical properties of bone, mainly its toughness and stiffness [47]. Crosslinking can significantly increase the ultimate strength of tissues composed of collagen fibers [48]. In this work, samples subjected to TnBP treatment also had higher ultimate strength than untreated samples. Cartmell and Dunn [3] also observed an increase in strength and modulus in tendons decellularized with 2% (v/v) TnBP, with no changes found for elongation at break.

The samples that underwent $scCO_2$ treatment had a significant increase in the Young's modulus compared to the untreated samples (66.24 MPa for 1 h and 65.94 MPa for 3 h). This increase in modulus was the highest observed among all treatments. The most likely explanation for this increase is that $scCO_2$ processing is known to cause water loss, which severely impacts values for both Young's modulus and ultimate strength [5,6]. The results obtained for the Young modulus appear in contradiction with previous studies that found no differences in mechanical parameters after $scCO_2$-based sterilization treatments [19,21]. However, these studies involved more complex protocols with several additional process steps (such as immersion in solutions of hydrogen peroxide, sodium hydroxide or ethanol), and in some cases exposure to gamma radiation, making a direct comparison of results difficult [18,19,21]. An increase in modulus after $scCO_2$ treatment, with or without co-solvent, has been reported in studies done in different tissues [5,6,10]. In this work, all samples were hydrated after decellularization treatment for 30 min, but a more extensive period of rehydration might be necessary to mitigate the effects of dehydration. Alternatively, future studies could incorporate the method developed by Casali et al. to maintain scaffold hydration levels while using $scCO_2$-based decellularization treatment [6]. An increase in the extensibility was detected for samples subjected to the 3 h protocol variant, as they sustained more strain before yield. It is possible that the alterations to the microstructure observed in micro-CT imagining were the cause of this change. No significant differences in the ductility were observed between untreated and $scCO_2$-treated samples, as elongation at break remained consistent.

The samples subjected to the $scCO_2$ using TnBP as co-solvent were generally found to have an increased modulus and ultimate strength than untreated samples. The increase in modulus was less after both $scCO_2$ treatments. It is possible that the addition of TnBP may have reduced the degree of water loss of the samples. However, the differences in modulus for these treatments were not considered significant. Additionally, samples treated with $scCO_2$-0.1% TnBP for 3 h and

Table 3
Young's Modulus, Ultimate Strength, and elongation at yield and break values were obtained for each treatment group. Young's Modulus and Ultimate Strength are presented as mean ± standard deviation.

Treatment	Young's Modulus (MPa)	Ultimate Strength (MPa)	Ɛ at Yield (%)	Ɛ at Break (%)
Untreated	47.61 ± 4.25	4.00 ± 0.61	20 ± 2.4	68 ± 6.9
TnBP 48 h	57.31 ± 3.66*	7.01 ± 0.81*	27 ± 7.3*	68 ± 9.8
$scCO_2$ 1 h	66.24 ± 8.10*	7.81 ± 1.15*	25 ± 5.3	62 ± 6.3
$scCO_2$ 3 h	65.94 ± 6.39*	7.35 ± 1.40*	26 ± 4.8*	70 ± 3.3
$scCO_2$-0.1% TnBP 1 h	62.70 ± 6.70*	7.01 ± 0.71*	22 ± 4.3	69 ± 5.4
$scCO_2$-0.1% TnBP 3 h	62.83 ± 4.41*	8.50 ± 1.85*	29 ± 6.4*	79 ± 8.2*
$scCO_2$-1% TnBP 1 h	61.21 ± 3.29*	8.88 ± 1.29*	26 ± 3.0*	80 ± 4.0*
$scCO_2$-1% TnBP 3 h	50.24 ± 4.20	7.53 ± 0.87*	24 ± 3.3	84 ± 1.7*

Significant differences between untreated and treated samples are indicated with a *$p \leq 0.05$ as compared by independent samples *t*-tests.

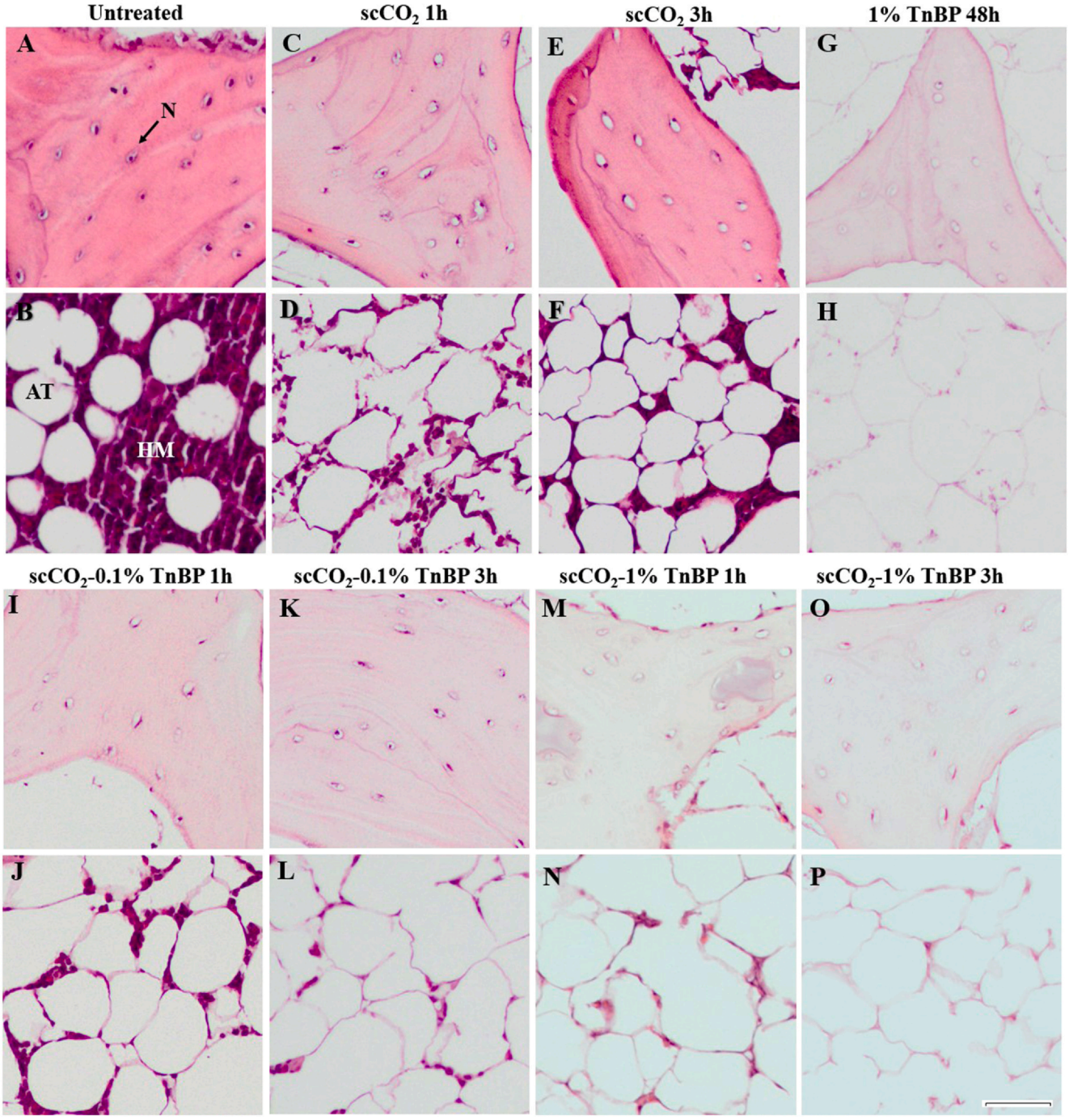

Fig. 7. Histological Analysis of Bone Samples: H&E staining of untreated and treated samples (10x) of (A,B) Untreated; (C,D) 1% TnBP treatment; (E,F) $scCO_2$ treatment for 1 h and (I,J) 3 h; (G,H) $scCO_2$-TnBP treatment for 1 h and (K,L) 3 h. Highlights: **(AT)** Adipose tissue; **(HM)** Hemopoietic marrow; **(N)** Cell nuclei. The scale bar indicates 50 μm.

$scCO_2$-1% TnBP for 1 h had superior ultimate strength than that observed for all other treatments. Values for elongation at yield and elongation at break were significantly higher in samples subjected to $scCO_2$-0.1% TnBP for 3 h and $scCO_2$-1% TnBP for 1 h compared to untreated samples. This increase in extensibility may be due to alterations to the microstructure of these samples, as observed in micro-CT images. As for the increased values for elongation at break, these appear to be correlated to the prolonged exposure of these samples to a high concentration (1%) of TnBP during $scCO_2$ treatment. Additionally, the samples subjected to $scCO_2$-1% TnBP for 3 h appeared to have lower stiffness and extensibility than samples subjected to other treatments, but similar to untreated samples.

4.3. Decellularization efficacy

The decellularization efficacy was proved by the reduction of DNA content at least 90% compared to native trabecular bone. The highest degree of DNA removal was found after samples were subjected to a 48-hours immersion in 1% TnBP (approximately 97%), resulting in a concentration of 0.216 μg of DNA per mg of dry ECM. The $scCO_2$ protocol resulted in a 66% (2.36 μg/mg) and 72% (1.98 μg/mg) reduction of DNA content for 1 h and 3 h of treatment, respectively. Histological analysis also confirmed that a significant amount of cellular content remained in the tissue after treatment (Fig. 7c-f). The high amount of residual cellular content may help explaining why these samples had a

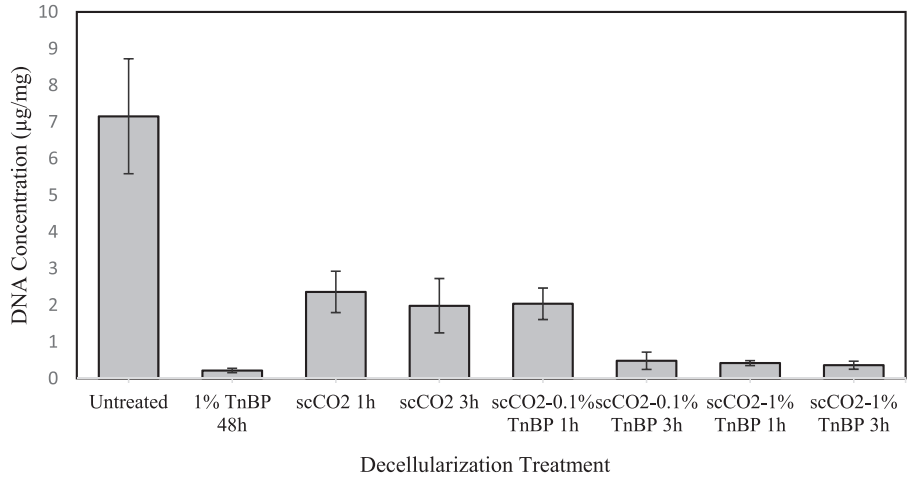

Fig. 8. DNA Concentration: Mean DNA Concentration (µg/mg) present in samples after each decellularization treatment. Error bars display standard deviation error for all mean values.

red hue, and suffered less discoloration than samples treated with $scCO_2$-TnBP or 1% TnBP. The solvent power of CO_2 decreases with increased compound polarity and molecular weight [49,50], as such "dry" scCO2 treatment has limited capability to remove biomolecules such as proteins or DNA. This outcome was similar to the results of Casali et al. [6], where the use of $scCO_2$ alone led to a decrease in DNA around 50%, which was insufficient for the purposes of decellularization. While in this work, pure $scCO_2$ led to a higher decrease of DNA content, the great porosity of trabecular bone and the pretreatment applied should account for the discrepancy. It has been hypothesized that $scCO_2$ leads to cell removal through to two possible mechanisms: i. The removal of cell components occurs during the supercritical stage, through extraction [5,6]. ii. the high pressure and supercritical environment cause cells to burst, while during depressurization, the rapid removal of CO_2 from the pressure chamber drags cellular material along with it [9]; Studies have shown that the effectiveness of cell removal is associated with the solvating power of CO_2, and increases with higher operating pressure or through modification with co-solvents [5,6,9], leading mainly to a mechanism behind of supercritical extraction, while pressure-induced cell death and dislodgement believed to play a smaller role. As CO_2 is a nonpolar molecule, it does not extensively interact with cellular materials that are charged [6,26], leading to a limited cell removal from the extracellular matrix. Therefore, the need for a co-solvent is highly justified.

The combined protocol of $scCO_2$-TnBP, the $scCO_2$-0.1% TnBP protocol resulted in a 71% reduction in DNA content after only 1 h of treatment time, and a 93% reduction after 3 h, resulting in a DNA concentration of 2.04 µg/mg and 0.482 µg/mg, respectively. The addition of TnBP marked a significant improvement in cell content removal, as compared to the $scCO_2$ protocol. Additionally, prolonging the length of exposure to this treatment to 3 h resulted in a significantly higher percentage of DNA removal, which is closer to the proposed minimum threshold of DNA content put forward by Crapo et al., which determined to be less than 0.05 µg of DNA per mg of ECM dry weight [26]. Nevertheless, this value is debatable, since more studies are needed to understand the immunogenic impact of biological residues according to the different decellularized tissue types. Histological analyses show that the extensive removal of marrow content occurred, particularly after the 3 h treatment.

After increasing TnBP concentration to 1%, the combined $scCO_2$-1% TnBP protocol resulted in a 94% decrease even after just one hour, resulting in a final concentration of 0.418 µg of DNA per mg of dry ECM, similar as those obtained for $scCO_2$-0.1% TnBP after 3 h treatment. Furthermore, while the extent of cell removal was similar between both treatments regarding marrow spaces, the $scCO_2$-1% TnBP for 1-hour treatment led to higher removal of cell nuclei from the lacunae in the trabeculae. However, while previously increasing treatment length had led to an increase in DNA removal of approximately 20%, the samples treated with $scCO_2$-1% TnBP for 3 h had 95% less DNA content than untreated samples (0.361 µg/mg), only slightly better than the 1-hour variant. Histological analysis revealed that marrow spaces were almost empty of nuclear content, however, this increase in the protocol length did not lead to higher removal of cell nuclei from the lacunae. These results suggest that more parameters, other than the amount of TnBP added to the pressure chamber, need to be re-adjusted in the combined $scCO_2$-TnBP protocol. Furthermore, increasing the length of exposure of trabecular bone samples to $scCO_2$-TnBP was not effective in achieving complete decellularization, and only led to marginal improvements for the $scCO_2$-1% TnBP protocol. These improvements could be achieved by using different parameters such as the pressure used during $scCO_2$ treatment, or addition of further steps to the protocol, such as additional washing.

Table 4
DNA concentration and corresponding percentage of DNA removal compared to untreated samples for each treatment group. DNA concentration is presented as the mean ± standard deviation.

Treatment	DNA Concentration (µg/mg)	Percentage of DNA Removal
Untreated	7.15 ± 1.57	–
1% TnBP 48 h	0.216 ± 0.060	97%
$scCO_2$ 1 h	2.36 ± 0.565	66%
$scCO_2$ 3 h	1.98 ± 0.743	72%
$scCO_2$-0.1% TnBP 1 h	2.04 ± 0.430	71%
$scCO_2$-0.1% TnBP 3 h	0.482 ± 0.236	93%
$scCO_2$-1% TnBP 1 h	0.418 ± 0.0689	94%
$scCO_2$-1% TnBP 3 h	0.361 ± 0.108	95%

The decellularization methodology here presented improved the overall time for decellularization as compared to other works in the literature. In particular, the use of $scCO_2$ allowed to reach a total period of 2–4 h. The majority of decellularization protocols to produce bone extracellular matrices takes 3 days up to 3 weeks [30,51–56]. Common methodologies for the decellularization of bone grafts involve immersion exposure to biological [51,52,56] or chemical agents [30,53,54], often followed by immersion in ethanol [51,53,55,57], for purposes of delipidation and dehydration. However, these immersions can extend for several hours or even days, due to its inefficiency in delivering decellularizing agents through tissues [26]. In a study by You and co-workers [8] a brief (30 min) $scCO_2$ treatment was introduced in their developed decellularization protocol of bone, to assist in the cleaning after the use of a detergent (Triton X-100). This strategy allowed to reduce the time of detergent removal as compared to previous works which needed the inclusion of long washing periods, which could be prolong into several days [53,55]. However, the use of a detergent is known to damage the bone structure and its biological content. The herein proposed $scCO_2$-based protocols are able to achieve fast decellularization of trabecular bone, with a total period of 2–4 h. Another major outcome of the present strategy is that it does not make use of detergents to achieve the required decellularization efficacy. In terms of ECM preservation, detergents as Triton X-100 may lead to the loss of elastin, GAGs, and disruption of collagen fibers, leading to an altered ultrastructure [2,3,58]. Sodium dodecyl sulfate, another commonly used detergent, can cause drastic alterations to the ECM due to the extensive damage to collagen and content and the removal of GAGs and growth factors [59–61]. These drawbacks can potentially lead to a mechanically compromised bone scaffold.

5. Conclusions

The present work investigated the potential of alternative methodologies using TnBP, supercritical carbon dioxide, or a combination of both as decellularization strategies for trabecular bone tissue. The use of TnBP in solution, instead of harsh chemicals such as detergents, has shown to be a promising methodology to better preserve the extracellular matrix, while ensuring the elimination of cellular content from the trabecular bone to a high extent. The mechanical properties of TnBP-treated samples increased, suggesting that TnBP could be promoting a degree of crosslinking to the collagen fibers. Since no previous works examining the effects of TnBP on bone tissue have yet been reported, further studies need to be developed to better understand the effect of TnBP on collagen and, consequently on the mechanical properties of bone.

The proposed treatment that used pure $scCO_2$ has proven to cause some removal of DNA content. However, the combined protocol of $scCO_2$-TnBP managed to decrease DNA content by at least 90%, inducing minimal changes to the microstructure of trabecular bone tissue, demonstrating its efficacy in the preservation of the extracellular matrix. Moreover, the presence of TnBP as co-solvent has led to a faster decellularization while using substantially lower concentrations of this reagent when compared to currently published literature. Not only is this approach more economically valuable, as it reduces the exposure time of tissues to potentially harmful treatments, opening room for new possibilities and future optimizations.

Funding

This work was supported by the Fundação para a Ciência e a Tecnologia (FCT) and Centro2020 [UIDB/04044/2020, UIDP/04044/2020, PAMI - ROTEIRO/0328/2013 (Nº 022158), POCI-01-0145-FEDER-31146, UID/Multi/50016/2019]; the European Union through PT2020 and Centro2020 [MATIS (CENTRO-01–0145-FEDER-000014)]; and Interreg V-A POCTEP Programme through FEDER funds from the European Union [0245_IBEROS_1_E].

Declaration of Competing Interest

The authors declare that they have no known competing financial interests or personal relationships that could have appeared to influence the work reported in this paper.

Acknowledgments

We acknowledge the staff at the Histology and Electron Microscopy platform at the Instituto de Investigaç ão e Inovaç ão em Saúde for their assistance in preparing histological specimens.

References

[1] N.F. Blair, T.J.R. Frith, I. Barbaric, Regenerative medicine: advances from developmental to degenerative diseases, Adv. Exp. Med. Biol. (2017) 225–239, https://doi.org/10.1007/978-3-319-60733-7_12
[2] R.W. Grauss, M.G. Hazekamp, S. van Vliet, A.C. Gittenberger-de Groot, M.C. DeRuiter, Decellularization of rat aortic valve allografts reduces leaflet destruction and extracellular matrix remodeling, J. Thorac. Cardiovasc. Surg. 126 (2003) 2003–2010, https://doi.org/10.1016/S0022-5223(03)00956-5
[3] J.S. Cartmell, M.G. Dunn, Effect of chemical treatments on tendon cellularity and mechanical properties, J. Biomed. Mater. Res. 49 (2000) 134–140, https://doi.org/10.1002/(SICI)1097-4636(200001)49:1<134::AID-JBM17>3.0.CO;2-D
[4] A. Porzionato, E. Stocco, S. Barbon, F. Grandi, V. Macchi, R. De Caro, Tissue-engineered grafts from human decellularized extracellular matrices: a systematic review and future perspectives, Int. J. Mol. Sci. 19 (2018) 4117, https://doi.org/10.3390/ijms19124117
[5] K. Sawada, D. Terada, T. Yamaoka, S. Kitamura, T. Fujisato, Cell removal with supercritical carbon dioxide for acellular artificial tissue, J. Chem. Technol. Biotechnol. 83 (2008) 943–949, https://doi.org/10.1002/jctb.1899
[6] D.M. Casali, R.M. Handleton, T. Shazly, M.A. Matthews, A novel supercritical CO_2-based decellularization method for maintaining scaffold hydration and mechanical properties, J. Supercrit. Fluids 131 (2018) 72–81, https://doi.org/10.1016/j.supflu.2017.07.021
[7] J. Antons, M. Marascio, P. Aeberhard, G. Weissenberger, N. Hirt-Burri, L. Applegate, P. Bourban, D. Pioletti, Decellularised tissues obtained by a CO_2-philic detergent and supercritical CO_2, Eur. Cells Mater. 36 (2018) 81–95, https://doi.org/10.22203/eCM.v036a07
[8] L. You, X. Weikang, Y. Lifeng, L. Changyan, L. Yongliang, W. Xiaohui, X. Bin, In vivo immunogenicity of bovine bone removed by a novel decellularization protocol based on supercritical carbon dioxide, Artif. Cells Nanomed. Biotechnol. 46 (2018) 334–344, https://doi.org/10.1080/21691401.2018.1457044
[9] S. Guler, B. Aslan, P. Hosseinian, H.M. Aydin, Supercritical carbon dioxide-assisted decellularization of aorta and cornea, Tissue Eng. Part C Methods 23 (2017) 540–547, https://doi.org/10.1089/ten.tec.2017.0090
[10] F.R. Halfwerk, J. Rouwkema, J.A. Gossen, J.G. Grandjean, Supercritical carbon dioxide decellularised pericardium: mechanical and structural characterisation for applications in cardio-thoracic surgery, J. Mech. Behav. Biomed. Mater. 77 (2018) 400–407, https://doi.org/10.1016/j.jmbbm.2017.10.002
[11] B. Topuz, G. Günal, S. Guler, H.M. Aydin, Use of supercritical CO_2 in soft tissue decellularization, Methods Cell Biol. 157 (2020) 49–79, https://doi.org/10.1016/bs.mcb.2019.10.012
[12] A. Gil-Ramírez, O. Rosmark, P. Spégel, K. Swärd, G. Westergren-Thorsson, A.K. Larsson-Callerfelt, I. Rodríguez-Meizoso, Pressurized carbon dioxide as a potential tool for decellularization of pulmonary arteries for transplant purposes, Sci. Rep. 10 (2020) 1–12, https://doi.org/10.1038/s41598-020-60827-4
[13] Y.-H. Huang, F.-W. Tseng, W.-H. Chang, I.-C. Peng, D.-J. Hsieh, S.-W. Wu, M.-L. Yeh, Preparation of acellular scaffold for corneal tissue engineering by supercritical carbon dioxide extraction technology, Acta Biomater. 58 (2017) 238–243, https://doi.org/10.1016/j.actbio.2017.05.060
[14] Y. Sun, V. Lovric, T. Wang, R.A. Oliver, W.R. Walsh, Effects of $SCCO_2$, gamma irradiation, and sodium dodecyl sulfate treatments on the initial properties of tendon allografts, Int. J. Mol. Sci. 21 (2020), https://doi.org/10.3390/ijms21051565
[15] J.K. Wang, B. Luo, V. Guneta, L. Li, S.E.M. Foo, Y. Dai, T.T.Y. Tan, N.S. Tan, C. Choong, M.T.C. Wong, Supercritical carbon dioxide extracted extracellular matrix material from adipose tissue, Mater. Sci. Eng. C 75 (2017) 349–358, https://doi.org/10.1016/j.msec.2017.02.002
[16] P.R. Chou, Y.N. Lin, S.H. Wu, S.D. Lin, P. Srinivasan, D.J. Hsieh, S.H. Huang, Supercritical carbon dioxide-decellularized porcine acellular dermal matrix combined with autologous adipose-derived stem cells: its role in accelerated diabetic wound healing, Int. J. Med. Sci. 17 (2020) 354–367, https://doi.org/10.7150/ijms.41155
[17] Y. Ling, W. Xu, L. Yang, C. Liang, B. Xu, Improved the biocompatibility of cancellous bone with compound physicochemical decellularization process, Regen. Biomater. 7 (2020) 443–451, https://doi.org/10.1093/rb/rbaa024
[18] J. Fages, A. Marty, C. Delga, J.S. Condoret, D. Combes, P. Frayssinet, Use of supercritical CO_2 for bone delipidation, Biomaterials 15 (1994) 650–656, https://doi.org/10.1016/0142-9612(94)90162-7
[19] D. Mitton, J. Rappeneau, R. Bardonnet, Effect of a supercritical CO_2 based treatment on mechanical properties of human cancellous bone, Eur. J. Orthop. Surg. Traumatol. 15 (2005) 264–269, https://doi.org/10.1007/s00590-005-0250-x

[20] J. Fages, E. Jean, P. Frayssinet, D. Mathon, B. Poirier, A. Autefage, D. Larzul, Bone allografts and supercritical processing: effects on osteointegration and viral safety, J. Supercrit. Fluids 13 (1998) 351–356, https://doi.org/10.1016/S0896-8446(98)00071-0
[21] L. Vastel, C. Masse, P. Mesnil, E. Crozier, F. Padilla, P. Laugier, D. Mitton, J.P. Courpied, Comparative ultrasound evaluation of human trabecular bone graft properties after treatment with different sterilization procedures, J. Biomed. Mater. Res. Part B Appl. Biomater. 90B (2009) 430–437, https://doi.org/10.1002/jbm.b.31302
[22] Y. Seo, Y. Jung, S.H. Kim, Decellularized heart ECM hydrogel using supercritical carbon dioxide for improved angiogenesis, Acta Biomater. 67 (2018) 270–281, https://doi.org/10.1016/j.actbio.2017.11.046
[23] M. Bottagisio, A.F. Pellegata, F. Boschetti, M. Ferroni, M. Moretti, A.B. Lovati, A new strategy for the decellularisation of large equine tendons as biocompatible tendon substitutes, Eur. Cells Mater. 32 (2016) 58–73, https://doi.org/10.22203/eCM.v032a04
[24] C.R. Deeken, A.K. White, S.L. Bachman, B.J. Ramshaw, D.S. Cleveland, T.S. Loy, S.A. Grant, Method of preparing a decellularized porcine tendon using tributyl phosphate, J. Biomed. Mater. Res. Part B Appl. Biomater. 96B (2011) 199–206, https://doi.org/10.1002/jbm.b.31753
[25] K. Suto, K. Urabe, K. Naruse, K. Uchida, T. Matsuura, Y. Mikuni-Takagaki, M. Suto, N. Nemoto, K. Kamiya, M. Itoman, Repeated freeze–thaw cycles reduce the survival rate of osteocytes in bone-tendon constructs without affecting the mechanical properties of tendons, Cell Tissue Bank. 13 (2012) 71–80, https://doi.org/10.1007/s10561-010-9234-0
[26] P.M. Crapo, T.W. Gilbert, S.F. Badylak, An overview of tissue and whole organ decellularization processes, Biomaterials 32 (2011) 3233–3243, https://doi.org/10.1016/j.biomaterials.2011.01.057
[27] T.W. Gilbert, T.L. Sellaro, S.F. Badylak, Decellularization of tissues and organs, Biomaterials 27 (2006) 3675–3683, https://doi.org/10.1016/j.biomaterials.2006.02.014
[28] B.D. Elder, D.H. Kim, K.A. Athanasiou, Developing an articular cartilage decellularization process toward facet joint cartilage replacement, Neurosurgery 66 (2010) 722–727, https://doi.org/10.1227/01.NEU.0000367616.49291.9F
[29] K. Chen, X. Lin, Q. Zhang, J. Ni, J. Li, J. Xiao, Y. Wang, Y. Ye, L. Chen, K. Jin, L. Chen, Decellularized periosteum as a potential biologic scaffold for bone tissue engineering, Acta Biomater. 19 (2015) 46–55, https://doi.org/10.1016/j.actbio.2015.02.020
[30] E. Abedin, R. Lari, N.M. Shahri, M. Fereidoni, Development of a demineralized and decellularized human epiphyseal bone scaffold for tissue engineering: a histological study, Tissue Cell 55 (2018) 46–52, https://doi.org/10.1016/j.tice.2018.09.003
[31] C. Guobao, L. Yonggang, Decellularized bone matrix scaffold for bone regeneration, Methods Mol. Biol. 1577 (2017) 239–254, https://doi.org/10.1002/bit.23024
[32] S.-I. Hong, Y.-R. Pyun, Membrane damage and enzyme inactivation of Lactobacillus plantarum by high pressure CO_2 treatment, Int. J. Food Microbiol. 63 (2001) 19–28, https://doi.org/10.1016/S0168-1605(00)00393-7
[33] J. Li, A. Wang, F. Zhu, R. Xu, X.S. Hu, Membrane damage induced by supercritical carbon dioxide in Rhodotorula mucilaginosa, Indian J. Microbiol. 53 (2013) 352–358, https://doi.org/10.1007/s12088-013-0373-4
[34] L. Polo-Corrales, M. Latorre-Esteves, J.E. Ramirez-Vick, Scaffold design for bone regeneration, J. Nanosci. Nanotechnol. 14 (2014) 15–56, https://doi.org/10.1166/jnn.2014.9127
[35] I. Marcos-Campos, D. Marolt, P. Petridis, S. Bhumiratana, D. Schmidt, G. Vunjak-Novakovic, Bone scaffold architecture modulates the development of mineralized bone matrix by human embryonic stem cells, Biomaterials 33 (2012) 8329–8342, https://doi.org/10.1016/j.biomaterials.2012.08.013
[36] R. Oftadeh, M. Perez-Viloria, J.C. Villa-Camacho, A. Vaziri, A. Nazarian, Biomechanics and mechanobiology of trabecular bone: a review, J. Biomech. Eng. 137 (2015), https://doi.org/10.1115/1.4029176
[37] A.R. Amini, D.J. Adams, C.T. Laurencin, S.P. Nukavarapu, Optimally porous and biomechanically compatible scaffolds for large-area bone regeneration, Tissue Eng. Part A 18 (2012) 1376–1388, https://doi.org/10.1089/ten.tea.2011.0076
[38] V. Karageorgiou, D. Kaplan, Porosity of 3D biomaterial scaffolds and osteogenesis, Biomaterials 26 (2005) 5474–5491, https://doi.org/10.1016/j.biomaterials.2005.02.002
[39] G. Liu, J. Sun, Y. Li, H. Zhou, L. Cui, W. Liu, Y. Cao, Evaluation of partially demineralized osteoporotic cancellous bone matrix combined with human bone marrow stromal cells for tissue engineering: an in vitro and in vivo study, Calcif. Tissue Int. 83 (2008) 176–185, https://doi.org/10.1007/s00223-008-9159-9
[40] T.M. Keaveny, E.F. Morgan, G.L. Niebur, O.C. Yeh, Biomechanics of trabecular bone, Annu. Rev. Biomed. Eng. 3 (2001) 307–333, https://doi.org/10.1146/annurev.bioeng.3.1.307
[41] A.S.P. Lin, T.H. Barrows, S.H. Cartmell, R.E. Guldberg, Microarchitectural and mechanical characterization of oriented porous polymer scaffolds, Biomaterials 24 (2003) 481–489, https://doi.org/10.1016/S0142-9612(02)00361-7
[42] S.-H. Kim, J.-W. Shin, S.-A. Park, Y.K. Kim, M.S. Park, J.M. Mok, W.I. Yang, J.W. Lee, Chemical, structural properties, and osteoconductive effectiveness of bone block derived from porcine cancellous bone, J. Biomed. Mater. Res. 68B (2004) 69–74, https://doi.org/10.1002/jbm.b.10084
[43] F. Linde, I. Hvid, F. Madsen, The effect of specimen geometry on the mechanical behaviour of trabecular bone specimens, J. Biomech. 25 (1992) 359–368, https://doi.org/10.1016/0021-9290(92)90255-Y
[44] T.M. Keaveny, R.E. Borchers, L.J. Gibson, W.C. Hayes, Trabecular bone modulus and strength can depend on specimen geometry, J. Biomech. 26 (1993) 991–1000, https://doi.org/10.1016/0021-9290(93)90059-N
[45] P. Zioupos, Ageing human bone: factors affecting its biomechanical properties and the role of collagen, J. Biomater. Appl. 15 (2001) 187–229, https://doi.org/10.1106/5JUJ-TFJ3-JVVA-3RJ0
[46] S. Xing, C. Liu, B. Xu, J. Chen, D. Yin, C. Zhang, Effects of various decellularization methods on histological and biomechanical properties of rabbit tendons, Exp. Ther. Med. 8 (2014) 628–634, https://doi.org/10.3892/etm.2014.1742
[47] P. Garnero, The contribution of collagen crosslinks to bone strength, Bone Rep. 1 (2012) 182, https://doi.org/10.1038/bonekey.2012.182
[48] B. Depalle, Z. Qin, S.J. Shefelbine, M.J. Buehler, Influence of cross-link structure, density and mechanical properties in the mesoscale deformation mechanisms of collagen fibrils, J. Mech. Behav. Biomed. Mater. 52 (2015) 1–13, https://doi.org/10.1016/j.jmbbm.2014.07.008
[49] J.M. Del Valle, J.M. Aguilera, Review: high pressure CO_2 extraction. Fundamentals and applications in the food industry, Food Sci. Technol. Int. 5 (1999) 1–24, https://doi.org/10.1177/108201329900500101
[50] F. Sahena, I.S.M. Zaidul, S. Jinap, A.A. Karim, K.A. Abbas, N.A.N. Norulaini, A.K.M. Omar, Application of supercritical CO_2 in lipid extraction – a review, J. Food Eng. 95 (2009) 240–253, https://doi.org/10.1016/j.jfoodeng.2009.06.026
[51] Y. Hashimoto, S. Funamoto, T. Kimura, K. Nam, T. Fujisato, A. Kishida, The effect of decellularized bone/bone marrow produced by high-hydrostatic pressurization on the osteogenic differentiation of mesenchymal stem cells, Biomaterials 32 (2011) 7060–7067, https://doi.org/10.1016/j.biomaterials.2011.06.008
[52] M.J. Sawkins, W. Bowen, P. Dhadda, H. Markides, L.E. Sidney, A.J. Taylor, F.R.A.J. Rose, S.F. Badylak, K.M. Shakesheff, L.J. White, Hydrogels derived from demineralized and decellularized bone extracellular matrix, Acta Biomater. 9 (2013) 7865–7873, https://doi.org/10.1016/j.actbio.2013.04.029
[53] C. Gardin, S. Ricci, L. Ferroni, R. Guazzo, L. Sbricoli, G. De Benedictis, L. Finotti, M. Isola, E. Bressan, B. Zavan, Decellularization and delipidation protocols of bovine bone and pericardium for bone grafting and guided bone regeneration procedures, PLOS One 10 (2015) e0132344, https://doi.org/10.1371/journal.pone.0132344
[54] D.J. Lee, S. Diachina, Y.T. Lee, L. Zhao, R. Zou, N. Tang, H. Han, X. Chen, C.-C. Ko, Decellularized bone matrix grafts for calvaria regeneration, J. Tissue Eng. 7 (2016) 2041731416680306, https://doi.org/10.1177/2041731416680306
[55] L. Karalashvili, N. Chichua, G. Menabde, L. Atskvereli, T. Grdzelidze, A. Machavariani, M. Zurmukhtashvili, K. Gogilashvili, Z. Kakabadze, Z. Chichua, Decellularized bovine bone graft for zygomatic bone reconstruction, Med. Case Rep. 4 (2018) 1–5, https://doi.org/10.21767/2471-8041.100087
[56] D. Bracey, T. Seyler, A. Jinnah, M. Lively, J. Willey, T. Smith, M. Van Dyke, P. Whitlock, A decellularized porcine xenograft-derived bone scaffold for clinical use as a bone graft substitute: a critical evaluation of processing and structure, J. Fish Biol. 9 (2018) 45, https://doi.org/10.3390/jfb9030045
[57] C.A. Smith, S.M. Richardson, M.J. Eagle, P. Rooney, T. Board, J.A. Hoyland, The use of a novel bone allograft wash process to generate a biocompatible, mechanically stable and osteoinductive biological scaffold for use in bone tissue engineering, J. Tissue Eng. Regen. Med. 9 (2015) 595–604, https://doi.org/10.1002/term.1934
[58] A. Roosens, P. Somers, F. De Somer, V. Carriel, G. Van Nooten, R. Cornelissen, Impact of detergent-based decellularization methods on porcine tissues for heart valve engineering, Ann. Biomed. Eng. 44 (2016) 2827–2839, https://doi.org/10.1007/s10439-016-1555-0
[59] M.-T. Kasimir, E. Rieder, G. Seebacher, G. Silberhumer, E. Wolner, G. Weigel, P. Simon, Comparison of different decellularization procedures of porcine heart valves, Int. J. Artif. Organs 26 (2003) 421–427, https://doi.org/10.1177/039139880302600508
[60] E.G. Bodnar, E. Olsen, R. Florio, J. Dobrin, Damage of porcine aortic valve tissue caused by the surfactant sodiumdodecylsulphate, Thorac. Cardiovasc. Surg. 34 (1986) 82–85, https://doi.org/10.1055/s-2007-1020381
[61] D.W. Courtman, C.A. Pereira, V. Kashef, D. McComb, J.M. Lee, G.J. Wilson, Development of a pericardial acellular matrix biomaterial: biochemical and mechanical effects of cell extraction, J. Biomed. Mater. Res. 28 (1994) 655–666, https://doi.org/10.1002/jbm.820280602